Fingerprints Hot Paper

DOI: 10.1002/anie.201305980

Nanoplasmonic Imaging of Latent Fingerprints and Identification of Cocaine**

Kun Li, Weiwei Qin, Fan Li, Xingchun Zhao, Bowei Jiang, Kun Wang, Suhui Deng, Chunhai Fan, and Di Li**

Fingerprints are impressions of the friction ridges of all or any part of a human finger. When a finger touches a surface, eccrine sweat, together with oily substances picked up by the finger, forms an impression of the finger's ridge pattern.[1] Such an impression is known as a latent fingerprint (LFP) for its invisibility to the naked eye. The uniqueness and invariableness of an individual's fingerprint have long been recognized as important physical personal identification, and is hence widely used in individual credentials, access control, and forensic investigation.[2] On the other hand, researchers have realized that fingerprints carry more biological information about individuals than just their identity.[2] The secretions, skin oils, and dead cells in LFPs contain residues of various chemicals and their metabolites present in the human body. These can be detected and used for forensic purposes. Therefore, the imaging of LFPs has found new applications in forensic fields, such as identifying drugs and drug metabolites, residues of explosives, and other secreted chemicals.[3] For this purpose, there has been an intense interest to develop enhanced LFP imaging methods[4] with various spectroscopic and microscopic techniques, for example, mass spectrometry,[4a,b] fluorescence spectroscopy,[4c,d] vibrational spectroscopy (infrared[4e] and Raman[4f]), electrochemiluminescence,[4g] and scanning electrochemical microscopy.[4h,i] Herein, we report a conceptually new nanoplasmonic approach to provide high-resolution dark-field microscopy (DFM) images of LFPs, as well as the ability to identify cocaine in LFPs by using aptamer-bound Au nanoparticles (Au NPs) as imaging and recognition probes.

Fingerprint friction ridges are generally described in a hierarchical order at three different levels, namely, level 1 (pattern), level 2 (minutia points), and level 3 (pores and ridge contours).[5] Currently used, commercialized, automated fingerprint-identification systems rely only on level 1 and level 2 features, and thus suffer from poor accuracy when the fingerprint is of low quality. Hence, new imaging methods for LFPs with high resolution are urgently needed. Although the above-mentioned new methods have been employed in forensic investigations, there remains a high demand for simple, rapid, user-friendly, cost-effective, and nondestructive methods for the imaging of LFPs and the detection of important chemical and biological analytes. Compared with previously reported methods, localized surface plasmon resonance (LSPR) of coinage-metal nanoparticles shows great potential for imaging because of its high intensity, nonblinking, optical stability,[6] and particularly its response depending on the size and local dielectric environment, thus making them particularly suitable for LFP imaging and molecular recognition in LFP.[7]

Au NPs have been used as enhancers for LFP imaging in a multimetal deposition (MMD) method.[8] The principle of MMD is the deposition of Au NPs on the finger secretions followed by silver staining. Although MMD has many advantages, it still suffers from several drawbacks; it is labor intensive, its accuracy is poorer, and it provides only gray- or black-colored images. Moreover, MMD can only visualize LFPs, but is unable to detect analytes of interest in LFPs. Recently, several modified versions of MMD were developed to realize both imaging and detection.[9] For example, Russell and co-workers modified Au NPs with an antibody that is specific to cotinine, the major metabolite of nicotine.[4c] After incubation of these antibody/Au NPs conjugates on a fingerprint collected on a glass slide and then with an organic-dye-labeled secondary antibody fragment, a high-resolution LFP image of an individual cigarette smoker was successfully collected by a fluorescence stereomicroscope. Even in these modified MMD methods, however, Au NPs were used only as "glues" that attached to LFPs and "carriers" of recognition probes and signal molecules (organic dye, quantum dots, or Raman tags); the LSPR properties of Au NPs are largely ignored. The advent of DFM combined with plasmonic resonance Rayleigh scattering (PRRS) spectroscopy in the last decade has provided a powerful means to directly image true colors of the light scattered from single plasmonic nanoparticles.[10] Indeed, several nanoplasmonic biosensing and imaging systems have been developed by DFM.[11] For example, previous studies have indicated that DFM could record the green-to-red color change of the scattered light of Au NPs during analyte-induced aggregation.[11c] This motivated us to develop a DFM assay to image LFPs and identify

[*] K. Li, W. W. Qin, F. Li, Dr. K. Wang, Dr. S. H. Deng, Prof. C. Fan, Prof. D. Li
Division of Physical Biology & Bioimaging Center, Shanghai Synchrotron Radiation Facility, Shanghai Institute of Applied Physics, Chinese Academy of Sciences
Shanghai 201800 (China)
E-mail: fchh@sinap.ac.cn
lidi@sinap.ac.cn
Prof. X. Zhao, Dr. B. Jiang
Institute of Forensic Science, Ministry of Public Security
Beijing (China)

[**] This work was supported by the National Basic Research Program of China (973 program, 2013CB932803, 2012CB825800, and 2013CB933800), the National Natural Science Foundation of China (21075128, 21227804, and 21222508), and the Shanghai Municipal Commission for Science and Technology (13QH1402300).

Supporting information for this article is available on the WWW under http://dx.doi.org/10.1002/anie.201305980.

cocaine in LFPs based on the cocaine-induced aggregation of aptamer-bound Au NPs.

The principle of our strategy is outlined in Figure 1. DFM is used to record the LSPR of Au NPs that attached to LFPs, thus providing a colorful image of LFPs. We modified two

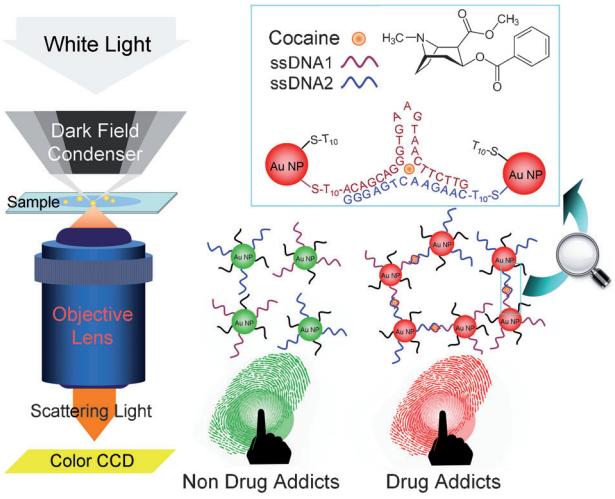

Figure 1. Principle of nanoplasmonic imaging of LFPs and identification of cocaine in LFPs by DFM.

Au NPs with rationally engineered cocaine-specific aptamers; thereby the presence of cocaine in LFPs could induce the aggregation of Au NPs, resulting in true color changes of the scattered light in DFM images. Briefly, Au NPs with a diameter of 50 nm were used as both imaging and recognition probes. A cocaine-specific aptamer was rationally cut into two pieces, which were then attached to different Au NPs by Au–S chemistry, respectively. Cocaine, working as a molecular linker, reassembles the two pieces of single-stranded DNA (ssDNA) into the intact aptamer tertiary structure, resulting in the aggregation of the Au NPs probes (Figure 1, inset).

The aggregation-induced red-to-blue absorption color changes of Au NPs have already been used as readout in aptasensors.[12] For example, Liu and Lu,[13a] and our group[13b,c] have independently reported solution-phase aptasensors for cocaine that rely on the cocaine-induced aggregation and deaggregation of aptamer-bound Au NPs.[13] Herein, we adapted this strategy to LSPR scattering in order to realize nanoplasmonic identification of cocaine in LFPs. The cocaine-specific aptamer reported by Stojanovic et al.[14] forms a stem-bulge-stem structure; however, this aptamer itself contains several secondary structures, even in the absence of cocaine, thus resulting in high background noise for aptasensors. After a careful analysis of the structure of the cocaine-specific aptamer, we divided it into two flexible ssDNA pieces (**1** and **2**; Figure 1, inset) with small sequence modifications to avoid interstrand binding.

A representative dark-field color image of a sebaceous LFP obtained by DFM with a 4× objective lens is shown in Figure 2 A. It should be noted that the size of LFPs is far beyond that of a condensed light spot, even with the lowest 4× objective lens. The dark-field image of the LFP was thus

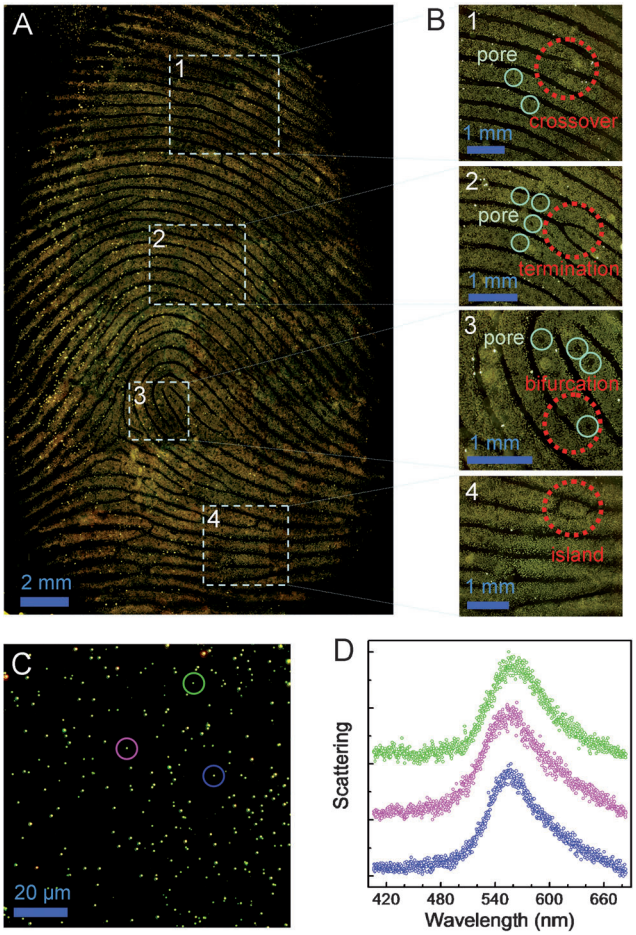

Figure 2. A) Dark-field image of a representative sebaceous LFP obtained with a 4× objective lens. B) Dark-field images of LFPs showing level 2 details including crossover (1), termination (2), bifurcation (3), and island (4), and level 3 details (pores in 1, 2, 3, and 4). C) Magnified dark-field image of a representative sebaceous LFP obtained with a 60× objective lens showing the presence of Au NPs. D) PRRS spectra of three randomly selected green-colored dots in Figure 1 C.

prepared by taking pictures of different regions of the LFP and their merging with the Photoshop software. The dark-field image of a sebaceous LFP displays a well-resolved ridge flow and pattern configuration with clear resolution between bright ridge and dark substrate. In addition to level 1 (ridge pattern) details, level 2 (ridge termination, lake, bifurcation, and crossover) and level 3 (pores with diameter of 50 μm) details of the LFP are also clearly observed (Figure 2 B), thus suggesting strong and specific interactions between Au NPs and sebaceous excretions. A control experiment indicates that LFPs are barely visible in the absence of Au NPs (Figure S1, Supporting Information), suggesting the effectiveness of Au NPs as contrast agents. In a high-magnification image obtained with a 60× objective lens, lots of green-colored dots are visible (Figure 2 C). The maximum wavelength (λ_{max}) of the scattered light of these green-colored dots is around 550 nm (Figure 2 D), which is the characteristic LSPR of Au NPs with diameters of 50 nm (Figure S2); therefore excluding the possibility of light scattered from dust in LFPs

and further confirming the presence of Au NPs attached to ridges. It is worth noting that this method is less effective for eccrine fingerprints, suggesting weaker physical adsorption between Au NPs and inorganic salts and amino acids in eccrine sweat.

We then used DFM to identify cocaine in LFPs. Briefly, solutions (10 μL) of cocaine with different concentrations (with the net mass of cocaine ranging from 150 ng to 30 μg) were drop-casted on fingers. After drying in air, the LFPs of the fingers were collected and then incubated with aptamer-bound Au NPs. Figure 3A shows the magnified dark-field images of LFPs containing different loadings of cocaine, obtained with a 60× objective lens. With the increase of the cocaine loading, we observed the gradual appearance of more red-colored dots along with the gradual disappearance of green-colored dots, thus indicating the aggregation of Au NPs. This finding was further confirmed by scanning electron microscopy (SEM; Figure S3). We also calculated λ_{max} of aggregates that contained different amounts of Au NPs using the Finite Difference Time Domain (FDTD) software (Figure S4), and found that even the aggregation of two Au NPs would result in a λ_{max} of 580 nm, corresponding to true orange-colored scattered light (Figure 3B). Therefore, we defined the orange- and red-colored dots in dark-field images with λ_{max} above 580 nm as cocaine-induced Au NP aggregates. In a randomly chosen ridge region in dark-field images containing about 300 individual Au NPs, we calculated the percentage of orange- and red-colored dots in the total dots. The relationship between the cocaine loading in LFPs and the percentage of orange- and red-colored dots in the total observable dots is shown in Figure 3C. We observed a loading-dependent red-shift of λ_{max}, which further confirmed the cocaine-induced aggregation of Au NPs. The minimally detectable cocaine loading in LFPs was calculated as 90 ng ($>3\sigma$).

We also carried out a control experiment to challenge the assay with two active cocaine metabolites, benzoyl ecgonine (BE) and ecgonine methyl ester (EME; chemical structures of BE and EME are shown in Figure S5), to demonstrate its selectivity toward cocaine. The selectivity of assays to identify drug addicts is of equal or even higher importance than the sensitivity, because a false positive signal may result in complicated law issues. Magnified dark-field images of clean (a), BE-loaded (b), EME-loaded (c), and cocaine-loaded LFPs (d) are shown in Figure 3D. Orange- and red-colored dots were observed only in cocaine-loaded LFPs. The responses of BE and EME were only slightly higher than that of the control (clean LFP), while greatly lower than that of cocaine (Figure 3E). The fact that cocaine, but not its metabolites, is detectable by this assay suggests that our strategy could also be used to differentiate between drug addicts and drug dealers who do not take drugs.

In summary, we have demonstrated a nanoplasmonic method to visualize LFPs by exploiting the LSPR property of aptamer-bound Au NPs. The level 2 and level 3 characteristic details of sebaceous LFPs could be clearly observed by DFM. Moreover, the cocaine-induced aggregation of Au NPs results in true green-to-red color change of the scattering in the dark-field image, thus providing a quasi-quantative method to

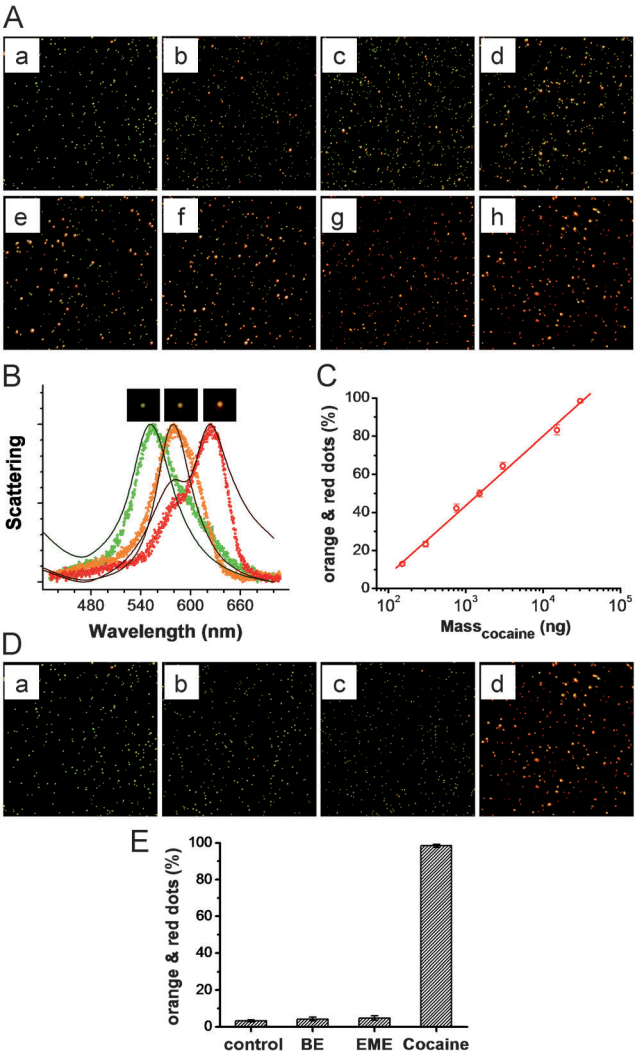

Figure 3. A) Magnified dark-field images of LFPs containing different loadings of cocaine. a) 0 g, b) 1.5×10^{-7} g, c) 3×10^{-7} g, d) 7.5×10^{-7} g, e) 1.5×10^{-6} g, f) 3×10^{-6} g, g) 1.5×10^{-5} g, and h) 3×10^{-5} g. B) Typical PRRS spectra of the green-, orange-, and red-colored dots (insets) experimentally obtained by spectrograph CCD (dotted lines). The solid lines are PRRS spectra obtained from FDTD simulation of a single Au NP, two-particle aggregation, and thirteen-particle aggregation, respectively. C) Calibration curve. Error bars represent standard deviations for measurements taken from at least three independent fingerprint areas. D) Magnified dark-field images of a) clean, b) BE-loaded, c) EME-loaded, and d) cocaine-loaded LFPs. E) Selectivity of the nanoplasmonic assay for cocaine over its metabolites. The mass of BE, EME, and cocaine was 30 μg in all experiments.

identify cocaine loadings in LFPs. Our dark-field nanoplasmonic strategy possesses several advantages. First, this method enables rapid, simple, and non-destructive visualization of LFPs, as well as the identification of level 2 and level 3 details. Meanwhile, DFM is much cheaper compared with other microscopic and spectroscopic instruments used for the imaging of LFPs, and hence is cost-effective in forensic applications. Second, the background view in DFM is dark. As a result, the substrates onto which the LFPs are loaded are completely invisible in dark-field images, resulting in improved edge resolution of LFPs. Third, the LSPR of

Au NPs is much more intense than fluorescent and luminescent or electrochemiluminescent signals, and is nonblinking and optically stable against photobleaching, thus providing significantly intensified signals with improved signal-to-noise ratio, and enabling higher spatial resolution in the imaging of LFPs. Last but not least, our strategy uses aptamer-bound Au NPs as a probe with dual functionality, including both imaging and molecular recognition. Taking into account the wide availability of aptamer libraries, our strategy could be in principle a generic platform for the identification of any small molecules or proteins in LFPs that have specific aptamers. Most promisingly, Au NPs are known for their high cellular uptake without apparent cell toxicity, and are indeed found in many in vivo applications.[15] Thus our LFP imaging strategy might one day be used in diagnostics in the examination of nanoplasmonic signals from rationally designed Au NP in vivo probes that secrete from finger pores.

Received: July 10, 2013
Published online: September 13, 2013

Keywords: aptamers · cocaine · fingerprints · gold · nanoparticles

[1] H. Faulds, *Nature* **1880**, *22*, 605.
[2] P. Hazarika, D. A. Russell, *Angew. Chem.* **2012**, *124*, 3582; *Angew. Chem. Int. Ed.* **2012**, *51*, 3524.
[3] a) X. N. Shan, U. Patel, S. P. Wang, R. Iglesias, N. J. Tao, *Science* **2010**, *327*, 1363; b) P. Hazarika, S. M. Jickells, K. Wolff, D. A. Russell, *Angew. Chem.* **2008**, *120*, 10321; *Angew. Chem. Int. Ed.* **2008**, *47*, 10167.
[4] a) D. R. Ifa, N. E. Manicke, A. L. Dill, G. Cooks, *Science* **2008**, *321*, 805; b) S. Y. Yang, C. F. Wang, S. Chen, *Angew. Chem.* **2011**, *123*, 3790; *Angew. Chem. Int. Ed.* **2011**, *50*, 3706; c) R. Leggett, E. E. Lee-Smith, S. M. Jickells, D. A. Russell, *Angew. Chem.* **2007**, *119*, 4178; *Angew. Chem. Int. Ed.* **2007**, *46*, 4100; d) P. Hazarika, S. M. Jickells, K. Wolff, D. A. Russell, *Anal. Chem.* **2010**, *82*, 9150; e) C. Ricci, S. Bleay, S. G. Kazarian, *Anal. Chem.* **2007**, *79*, 5771; f) W. Song, Z. Mao, X. J. Liu, Y. Lu, Z. S. Li, B. Zhao, L. H. Lu, *Nanoscale* **2012**, *4*, 2333; g) L. R. Xu, Y. Li, S. Z. Wu, X. H. Liu, B. Su, *Angew. Chem.* **2012**, *124*, 8192; *Angew. Chem. Int. Ed.* **2012**, *51*, 8068; h) M. Q. Zhang, H. H. Girault, *Electrochem. Commun.* **2007**, *9*, 1778; i) M. Zhang, H. H. Girault, *Analyst* **2009**, *134*, 25.
[5] A. Robert Hillman, R. M. Brown, K. S. Ryder, C. Fullarton, M. W. A. Skoda, R. M. Dalgliesh, E. Watkins, C. Beebee, R. Barker, A. Glidle, *Faraday Discuss.* **2013**, DOI: 10.1039/C3FD00053B.
[6] a) Y. Li, C. Jing, L. Zhang, Y. T. Long, *Chem. Soc. Rev.* **2012**, *41*, 632; b) V. Myroshnychenko, J. Rodriguez-Fernandez, I. Pastoriza-Santos, A. M. Funston, C. Novo, P. Mulvaney, L. M. Liz-Marzan, F. J. G. de Abajo, *Chem. Soc. Rev.* **2008**, *37*, 1792; c) S. P. Song, Y. Qin, Y. He, Q. Huang, C. H. Fan, H. Y. Chen, *Chem. Soc. Rev.* **2010**, *39*, 4234; d) Y. D. Jin, *Adv. Mater.* **2012**, *24*, 5153; e) D. Li, S. P. Song, C. H. Fan, *Acc. Chem. Res.* **2010**, *43*, 631.
[7] a) S. Eustis, M. A. El-Sayed, *Chem. Soc. Rev.* **2006**, *35*, 209; b) B. Pelaz, S. Jaber, D. J. de Aberasturi, V. Wulf, T. Aida, J. M. de La Fuente, J. Feldmann, H. E. Gaub, L. Josephson, C. R. Kagan, N. A. Kotov, L. M. Liz-Marzan, H. Mattoussi, P. Mulvaney, C. B. Murray, A. L. Rogach, P. S. Weiss, I. Willner, W. J. Parak, *ACS Nano* **2012**, *6*, 8468; c) S. Lal, S. Link, N. J. Halas, *Nat. Photonics* **2007**, *1*, 641.
[8] a) M. J. Choi, A. M. McDonagh, P. Maynard, C. Roux, *Forensic Sci. Int.* **2008**, *179*, 87; b) A. Becue, C. Champod, P. Margot, *Forensic Sci. Int.* **2007**, *168*, 169.
[9] X. Spindler, O. Hofstetter, A. M. McDonagh, C. Roux, C. Lennard, *Chem. Commun.* **2011**, *47*, 5602.
[10] a) J. Becker, O. Schubert, C. Sonnichsen, *Nano Lett.* **2007**, *7*, 1664; b) N. J. Halas, *Nano Lett.* **2010**, *10*, 3816; c) M. Grzelczak, L. M. Liz-Marzan, *Langmuir* **2013**, *29*, 4652; d) E. Ringe, B. Sharma, A. I. Henry, L. D. Marks, R. P. Van Duyne, *Phys. Chem. Chem. Phys.* **2013**, *15*, 4110.
[11] a) J. N. Anker, W. P. Hall, O. Lyandres, N. C. Shah, J. Zhao, R. P. Van Duyne, *Nat. Mater.* **2008**, *7*, 442; b) R. de La Rica, M. M. Stevens, *Nat. Nanotechnol.* **2012**, *7*, 821; c) X. X. Zheng, Q. Liu, C. Jing, Y. Li, D. Li, W. J. Luo, Y. Q. Wen, Y. He, Q. Huang, Y.-T. Long, C. H. Fan, *Angew. Chem.* **2011**, *123*, 12200; *Angew. Chem. Int. Ed.* **2011**, *50*, 11994; d) L. Zhang, Y. Li, D. W. Li, C. Jing, X. Y. Chen, M. Lv, Q. Huang, Y.-T. Long, I. Willner, *Angew. Chem.* **2011**, *123*, 6921; *Angew. Chem. Int. Ed.* **2011**, *50*, 6789; e) L. Shi, C. Jing, W. Ma, D.-W. Li, J. E. Halls, F. Marken, Y.-T. Long, *Angew. Chem.* **2013**, *125*, 6127; *Angew. Chem. Int. Ed.* **2013**, *52*, 6011; f) G. Raschke, S. Kowarik, T. Franzl, C. Sonnichsen, T. A. Klar, J. Feldmann, A. Nichtl, K. Kurzinger, *Nano Lett.* **2003**, *3*, 935; g) C. Sönnichsen, B. M. Reinhard, J. Liphardt, A. P. Alivisatos, *Nat. Biotechnol.* **2005**, *23*, 741; h) Z. D. Wang, J. Q. Zhang, J. M. Ekman, P. J. A. Kenis, Y. Lu, *Nano Lett.* **2010**, *10*, 1886.
[12] a) J. W. Liu, Z. H. Cao, Y. Lu, *Chem. Rev.* **2009**, *109*, 1948; b) I. Willner, M. Zayats, *Angew. Chem.* **2007**, *119*, 6528; *Angew. Chem. Int. Ed.* **2007**, *46*, 6408; c) J. S. Lee, M. S. Han, C. A. Mirkin, *Angew. Chem.* **2007**, *119*, 4171; *Angew. Chem. Int. Ed.* **2007**, *46*, 4093; d) H. Xu, B. Liu, Y. Chen, *Microchim. Acta* **2012**, *177*, 89 – 94; e) B. Liu, L. Lu, E. Hua, S. Jiang, G. Xie, *Microchim. Acta* **2012**, *178*, 163 – 170; f) Z. Q. Zhu, Y. Y. Su, J. Li, D. Li, J. Zhang, S. P. Song, Y. Zhao, G. X. Li, C. H. Fan, *Anal. Chem.* **2009**, *81*, 7660 – 7666; g) J. L. Wang, H. S. Zhou, *Anal. Chem.* **2008**, *80*, 7174 – 7178; h) L. H. Guo, A. R. Ferhan, K. Lee, D. H. Kim, *Anal. Chem.* **2011**, *83*, 2605 – 2612.
[13] a) J. W. Liu, Y. Lu, *Angew. Chem.* **2006**, *118*, 96; *Angew. Chem. Int. Ed.* **2006**, *45*, 90; b) J. Zhang, L. H. Wang, D. Pan, S. P. Song, F. Y. C. Boey, H. Zhang, C. H. Fan, *Small* **2008**, *4*, 1196; c) F. Li, J. Zhang, X. N. Cao, L. H. Wang, D. Li, S. P. Song, B. C. Ye, C. H. Fan, *Analyst* **2009**, *134*, 1355.
[14] M. N. Stojanovic, P. de Prada, D. W. Landry, *J. Am. Chem. Soc.* **2001**, *123*, 4928.
[15] A. A. Mohamed, *Gold Bull.* **2011**, *44*, 71.

